Journal of Electrical Engineering, Vol. 74, No. 4, 2023, pp. 282-292

sciendo
PAPER

Conformable fractional-order derivative based adaptive FitzHugh-Nagumo neuron model

Ertuğrul Karakulak

Various neuron models have been proposed and are extensively examined in the scientific literature. The FitzHugh-Nagumo neuron model is one of the most well-known and studied models. The FitzHugh-Nagumo model is not biologically consistent but operationally simple. A fractional-order derivative is described as a derivative with a non-integer order. Caputo, Grünwald-Letnikov, and Riemann-Liouville are some of the well-known fractional order derivatives. However, a simple fractional-order derivative called the conformable fractional-order derivative has been proposed in the literature and it is much simpler to use. In literature, there are already neuron models with fractional-order derivatives. In this study, a FitzHugh-Nagumo model circuit with a conformable fractional derivative capacitor and conformable fractional derivative inductor is proposed. The proposed circuit is modelled, and its simulation results are given. The simulation results reveal that the model circuit shows both slow and fast adaptation in firing frequency under sustained current stimulation.

Keywords: conformable fractional derivative, FitzHugh-Nagumo neuron model, neuron model, neural adaptation

1. Introduction

Biological neuron models represent the mathematical description of action potentials experienced in the neuron axon. The two main features expected from neuron models are biological consistency and mathematical simplicity [1]. The simplified neuron models are useful when the literal behaviour of neurons is not critical [2]. The FitzHugh-Nagumo (FHN) neuron model has been suggested in 1961 by Richard FitzHugh [3]. The circuit of the FHN model has been proposed by Jinichi Nagumo et al. in 1962 [4]. Their works have influenced many studies in the field of neuroscience [1,2]. Although the FHN model is not biologically consistent, it is mathematically simple [1-4]. It has a pair of differential equations to model action potentials in the neuron axon and it works as a relaxation oscillator [3,4]. The FHN model is a simplified 2D version of the Hodgkin-Huxley [5] neuron model. Although the Hodgkin-Huxley neuron model is one of the most consistent models with neuron physiology and electrophysiology, it is also one of the most detailed and complex neuron models. The Izhikevich neuron model, like the FHN model, has a nonlinearity and can model neuron behaviours pretty accurately [6]. The Izhikevich model is not inspired by neuron biophysics, but it reveals the spiking and bursting behaviour of cortical nerves [7]. One of the neuron models with the least computational complexity is the Integrate-and-fire (IF) model which has been proposed by Louis Lapicque [8]. In Lapicque's model, the cell membrane is modelled as a capacitor and the capacitor is discharged when the capacitor voltage exceeds a certain threshold voltage. This discharge stage is called "fire" and various Integrate-and-fire (IF) models have been proposed in the literature [9,10].

Neural adaptation or sensory adaptation can be simply defined as a decreased response of the neural system to a constant stimulus. Considering a biological neuron, the decrease in the number of spikes per second of the neuron membrane voltage in response to a constant stimulus can be called neural adaptation. This adaptation behaviour in a biological neuron is due to the calcium current in the cell membrane and the changes in the calcium concentration between the inside and outside of the cell [11-13]. There are two types of adaptation: fast and slow. Fast adaptation occurs in milliseconds, whereas slow adaptation can take minutes or even hours [13].

Fractional calculus or non-integer order calculus dates back to the Leibnitz era [14], but nowadays it attracts attention with its use in various fields such as mathematics, engineering, and neuroscience [15,16]. It is also a method that is successfully used in the modelling of complex systems [17]. The fractional-order derivative can simply be expressed as a derivative with a non-integer order. Various fractional-order derivative equations have been proposed in the literature. Some well-known examples of them are Caputo [18], Riemann–Liouville [19], and Grünwald-Letnikov [20]. Most of these equations make use of fractional-order integrals which are hard to evaluate. Khalil et al. proposed an equation, they named "Conformable Fractional-Order Derivative" (CFD) in 2014 [21], and Abdeljawad made final refinements in 2015 [22]. CFD simply consists of a first-order derivative multiplied by the fractional-order power of the function variable. CFD offers a physically interpretable solution for the fractional-order derivative and stands out for its simplicity. Due to its low complex features, it has become a hot research topic in the scientific literature [23,[24]. Fractional order derivatives have also been proposed for modelling neurons and neurological systems [25,26]. CFD has been proposed to re-examine and modify some of the known neuron models [27]. The FHN neuron model based on fractional order derivative (Grünwald-Letnikov [20] equation is used) has also been suggested [28]. However, to the best of our knowledge, no one has suggested a CFD-based FHN neuron model circuit yet. In this study, a CFD-based FHN neuron model is suggested, and its adaptation abilities are shown using simulations. Such a model offers richer dynamics than the FHN circuit.

Tekirdağ Namık Kemal University, Vocational School of Technical Sciences, Biomedical Device Technology Department,
59100 Tekirdağ, Turkey
ekarakulak@nku.edu.tr

https://doi.org/10.2478/jee-2023-0035, Print (till 2015) ISSN 1335-3632, On-line ISSN 1339-309X

This paper is organized as follows. In the second section, CFD, CFD capacitor, and CFD inductor are introduced. The FHN model circuit with a CFD capacitor and a CFD inductor is briefly explained in the third section. The simulation results are given in the fourth section. The paper is concluded with a conclusion section.

2. Conformable fractional derivative, CFD capacitor and CFD inductor

The fractional-order derivative can simply be expressed as a derivative with a non-integer order. Numerous methods have been proposed in the scientific literature for fractional-order derivatives [18-20]. Most of these methods are computationally complex. Khalil et al. proposed a simple and well-behaved fractional derivative naming it the "Conformable Fractional Derivative" [21]. Detailed information on CFD can be found in [21-23]. CFD can be expressed as

$$\frac{d^{\alpha}f(t)}{dt^{\alpha}} = f'(t)\,t^{(1-\alpha)} = \frac{df(t)}{dt}t^{(1-\alpha)}, \tag{1}$$

where α is the order of fractional derivative and it must be provided that $1 \geq \alpha > 0$. According to Eq. (1), multiplying the ordinary first-order derivative by $t^{(1-\alpha)}$ is sufficient to obtain CFD of αth order. It should be noted that CFD offers a physically interpretable solution for the fractional-order derivative and stands out for its simplicity [21-23].

A CFD capacitor and a CFD inductor have already been proposed in literature [29,30]. Capacitor current equation and inductor voltage equations have derivatives. Equation (2) and Eq. (3) show the capacitor current and inductor voltage formulas, respectively.

$$i_c(t) = C\frac{dv_c(t)}{dt}, \tag{2}$$

$$V_L(t) = L\frac{di_L(t)}{dt}, \tag{3}$$

where i_c is capacitor current, v_c is capacitor voltage, i_L is inductor current, v_L is inductor voltage, C is capacitance, and L is inductance respectively.

CFD capacitor current equation and CFD inductor voltage equations can be obtained by replacing the ordinary time derivative with CFD. Equation (4) and Eq. (5) show the CFD capacitor and CFD inductor constitutive laws respectively.

$$i_c = C_{\propto}\frac{d^{\propto}v}{dt^{\propto}} = (C_{\propto}t^{(1-\propto)})\frac{dv_c}{dt} \tag{4}$$

$$V_L = L_{\beta}\frac{d^{\beta}i_L}{dt^{\beta}} = (L_{\beta}t^{(1-\beta)})\frac{di_L}{dt} \tag{5}$$

where $C_{\propto}$ is the CFD capacitor capacitance, L_{β} is the CFD inductor inductance, α and β are the fractional order of the CFD capacitor and the CFD inductor respectively.

According to Eq. (4) and (5), the values of the capacitor and inductor have become time-variant and increase with time. The symbols of the CFD capacitor and the CFD inductor are shown in Fig. 1.

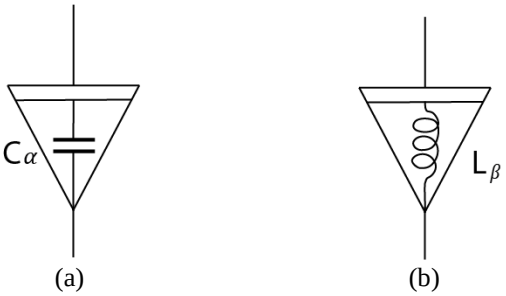

Fig. 1. (a) Symbol of the CFD capacitor and (b) symbol of the CFD inductor

3. FitzHugh-Nagumo model circuit with CFD capacitor and CFD inductor

The FHN model circuit is extensively examined and modified versions of the circuit are suggested in the scientific literature [28,31,32]. It is also an example of a relaxation oscillator and has the same properties as the two-dimensional Van Der Pol Oscillator [33, 34]. However, unlike the Van Der Pol oscillator, the FHN model needs an external excitation current. In addition, the FHN model is derived from the phase plane analysis of the Hodgkin-Huxley model. The basis of this neuron model is independent of the sodium and potassium diffusion behaviour in the neuron membrane. The model consists of two differential equations. One of them defines the membrane potential (Eq. (6)) and has a cubic nonlinearity. This equation has an external excitation current variable. The second differential equation defines the rate of the change of the recovery variable (Eq. (7)) and

has a linear dynamic structure. This equation provides slow negative feedback. The membrane potential equation of the FHN model is,

$$\frac{dv}{dt} = v - \frac{v^3}{3} - w + RI_{ext}, \tag{6}$$

where v is a membrane potential-like variable, w is the recovery variable of the model, I_{ext} is the external stimulus current of the model, and R is the external stimulus coefficient.

The recovery variable equation is given as,

$$\frac{dw}{dt} = \frac{v+a-bw}{\tau}, \tag{7}$$

where a, b, and τ are parameters which determine the duration and the fixed point of the recovery.

The Nagumo circuit can be seen in Fig. 2(a). The external current source is designated as I_{ext} in the circuit. The value v, which denotes the membrane potential, is equivalent to the capacitor voltage and the recovery variable (w) is the inductor current. The cubic parameter in the FitzHugh equations (Eq. (6)) is modelled with a tunnel diode.

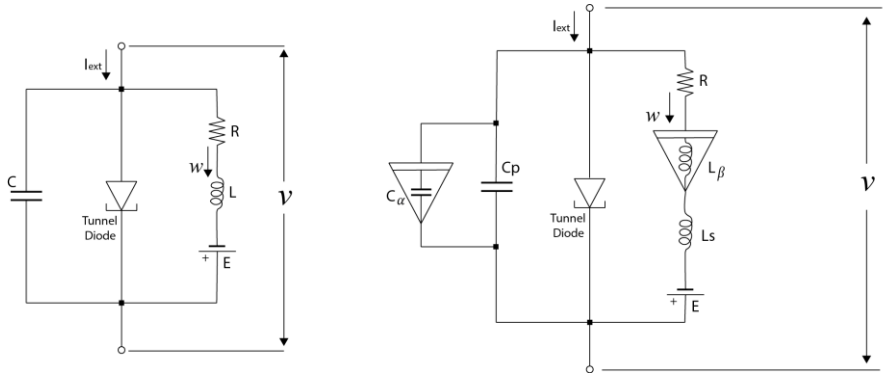

(a) (b)

Fig. 2. (a) Nagumo circuit and (b) The modified Nagumo circuit modified with a CFD capacitor and a CFD inductor

The Nagumo circuit in Fig. 2(a) is modified with a CFD capacitor and a CFD inductor to obtain the new FHN circuit shown in Fig. 2(b). For the circuit shown in Fig. 2(a), the capacitor current and the inductor voltage are obtained by Kirchhoff's current and voltage laws. Equation (8) and (9) describe the state space system of the FHN model.

$$C\frac{dv}{dt} = I_{ext} - w - f(v) \tag{8}$$

$$L\frac{dw}{dt} = v - wR + E \tag{9}$$

where R, L, C, and E denote resistance, inductance, capacitance, and the reverse voltage source, respectively. The DC voltage sources connected in reverse (E) in the Nagumo circuits represent the resting membrane potential (voltage) of a neuron which is in resting state. $f(v)$ is the function that expresses the current-voltage characteristic of the tunnel diode.

Equations (8) and (9) turn into FitzHugh equations given in Eq.s (6) and (7) with proper selection of the parameters. The CFD capacitor and the Linear Time-Invariant (*LTI*) capacitor are connected in parallel and the CFD inductor and the LTI inductor are connected in series for the modified FHN circuit as seen in Fig. 2(b). The equivalent capacitance of the CFD capacitor and the LTI capacitor connected in parallel and the equivalent inductance of the CFD inductor and the LTI inductor connected in series are given in Eqs. (10) and (11), respectively.

$$C_{eq}(t) = C_p + C_\propto t^{(1-\propto)} \tag{10}$$

$$L_{eq}(t) = L_s + L_\beta t^{(1-\beta)} \tag{11}$$

C_p is the capacitance of the LTI capacitor, L_s is the inductance of the LTI inductor, C_{eq} is the equivalent capacitance, and L_{eq} is the equivalent inductance.

Using the Kirchhoff's Laws, the state space system of the modified FHN model can be given as

$$\frac{dv}{dt} = \frac{I_{ext} - w - f(v)}{C_{eq}(t)} = \frac{I_{ext} - w - f(v)}{C_p + C_{\propto} t^{(1-\propto)}} \tag{12}$$

$$\frac{dw}{dt} = \frac{v - wR + E}{L_{eq}(t)} = \frac{v - wR + E}{L_s + L_{\beta} t^{(1-\beta)}} \tag{13}$$

As it can be seen in Eq. (12) and (13), both the rate of change of the membrane potential and the recovery variable have become time-variant due to the terms $t^{(1-\propto)}$ and $t^{(1-\beta)}$. Therefore, it is possible to obtain neural adaptation behaviour with this time dependency. But, in the absence of stimulation, the change in the behaviour of the model does not conform to the adaptation behaviour of the biologic neuron. In this case, the model must be modified so that the terms $t^{(1-\propto)}$ and $t^{(1-\beta)}$ should be modified to be reset to zero at the start of each excitation. The external excitation pulse given in Fig. 3 can be described as

$$I_{ext} = I_p\,[k]\big[u(t - t_{start}[k]) - u\big(t - t_{stop}[k]\big)\big], \tag{14}$$

where I_p is the magnitude of the external current, t_{start} is the start time of the pulse, t_{stop} is the stop time of the pulse and, $u()$ is the step function.

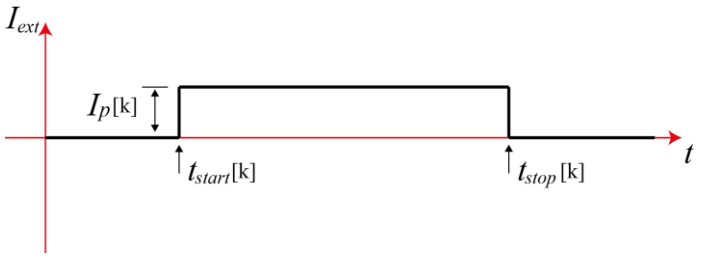

Fig. 3. The k[th] external excitation or stimulation pulse

In this case, t_{onset}, which is the start time of the k^{th} pulse, can be defined as

$$t_{onset}[k] = t_{start}[k] \tag{15}$$

Then, the CFD based FHN onset model can be given as

$$\frac{dv}{dt} = \frac{I_{ext} - w - f(v)}{C_{eq}(t)} = \frac{I_{ext} - w - f(v)}{C_p + C_{\propto}(t - t_{onset}[k])^{(1-\propto)}} \tag{16}$$

$$\frac{dw}{dt} = \frac{v - wR + E}{L_{eq}(t)} = \frac{v - wR + E}{L_s + L_{\beta}(t - t_{onset}[k])^{(1-\beta)}} \tag{17}$$

According to Eqs. (14) and (15) the terms $(t - t_{onset}[k])^{(1-\propto)}$ and $(t - t_{onset}[k])^{(1-\beta)}$ is reset to zero at the beginning of each excitation. Thus, the model's behaviour is prevented from changing during each stimulation and refractory period.

Simulink block diagram of the CFD-based FHN neuron model is given in Fig. 4. It has three subsystems which makes the preparation of the diagram easier and allows having modularity. Their internal structures are also shown in Fig. 4.

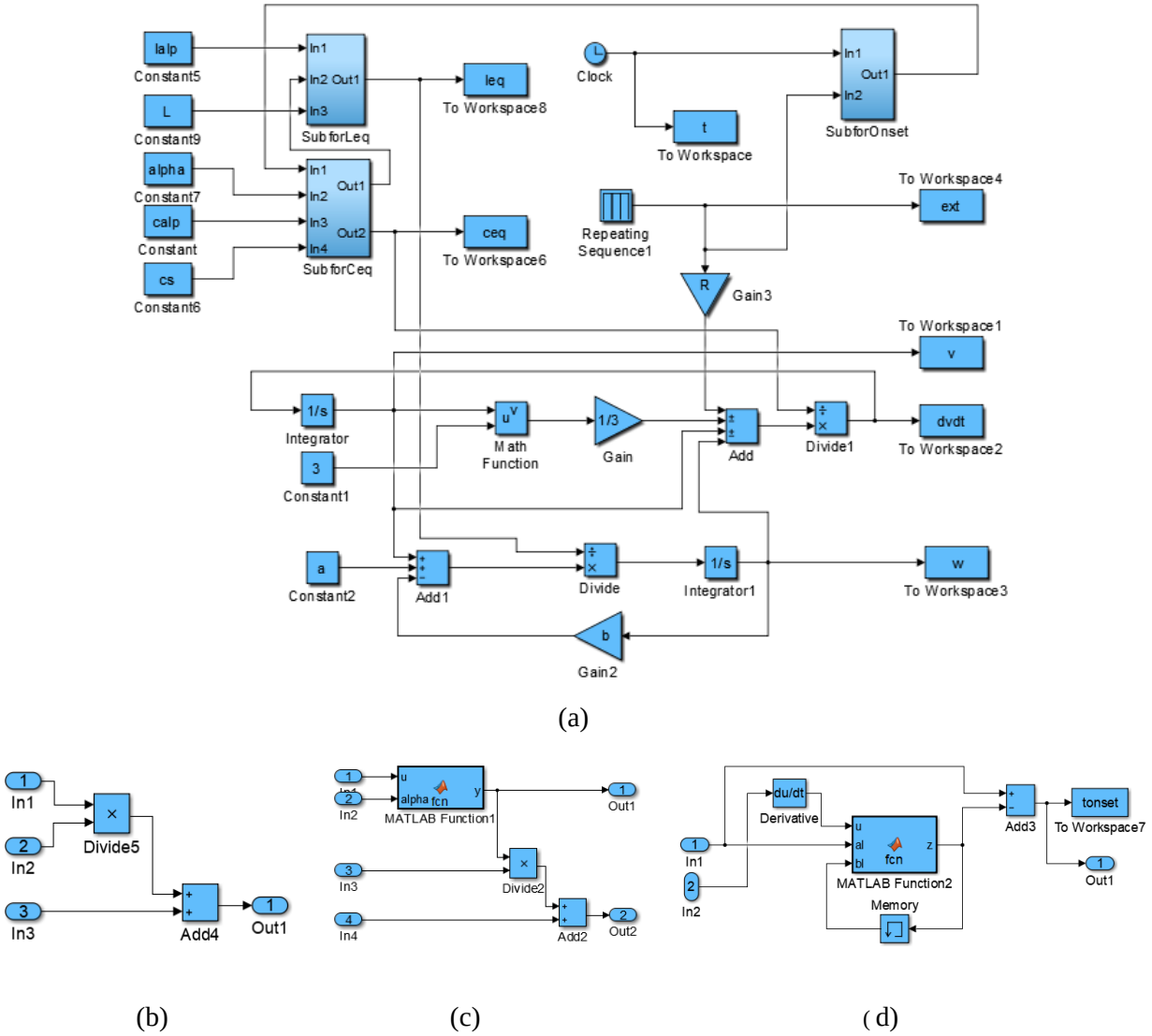

Fig. 4. (a) Simulink block diagram of the CFD based FHN neuron model, (b) The block diagram of the subsystem named *SubforLeq*, (c) The block diagram of the subsystem named *SubforCeq*, and (d) The block diagram of the subsystem named *SubforOnset.*

The block diagram of the subsystem named *SubforLeq*, which is used to calculate the equivalent inductance of series-connected L_s and L_β, is shown in Fig. 4b. The block diagram of the subsystem named *SubforCeq*, which includes blocks to calculate the equivalent capacitance of parallel connected capacitors C_p and C_α, is shown in Fig. 4c. This subsystem has a Matlab Function block which calculates the value of $t^{1-\propto}$. Therefore, using *SubforLeq* and *SubforCeq*, the equivalent capacitance and the equivalent inductance of the modified Nagumo circuit shown in Fig. 2b are obtained. The block diagram of the subsystem named *SubforOnset*, which is used to calculate the start time of the k^{th} pulse, $t_{onset}[k]$, is shown in Fig. 4d. This block also possesses a Matlab Function block which calculates the piecewise function given in Eq. (18).

$$z = \begin{cases} a_1, & u > 0 \\ b_1, & u \le 0 \end{cases} \tag{18}$$

4. Simulation results

The modified FHN circuit model is created with Simulink™ toolbox of Matlab™ and its simulation results are obtained. The parameters in Tab. 1 are chosen as simulation parameters. In addition to the parameters taken from the [33], C_α and L_β parameters are chosen as 5% of C_p and L_s parameters, respectively.

Table 1. Parameters of simulations

Parameters	*Values*
E	0.7 V
R	0.8 Ω
C	1 F
$C_{\propto}$	0.05 F/s$^{(1-\propto)}$
L	12.5 H
L_{β}	0.625 H/s$^{(1-\beta)}$

Parameters α and β are chosen as equal and the obtained simulation results are shown in Fig. 5-11. Simulations are made for 0.2, 0.4, 0.5, 0.6, and 0.8 values of α and β. When the α and β parameters are equal to 1, $(t-t_{onset}[k])^{(1-\propto)}$ and $(t-t_{onset}[k])^{(1-\beta)}$ multipliers become 1 and the proposed model turns into the ordinary FHN model. Therefore, no simulations have been made for these values. When the α and β parameter values are 0, the multipliers of $(t-t_{onset}[k])^{(1-\propto)}$and $(t-t_{onset}[k])^{(1-\beta)}$are equal to $(t-t_{onset}[k])$ and the CFD derivative is not defined as told in Section 2. For this reason, this value is also not used in the simulations. As seen in Fig. 5(a)-9(a), the curve shown in blue is the output voltage signal of the model and the other shown in red is the external excitation signal. The recovery variable signal of the model and the external excitation signal are shown in blue and red respectively in Fig. 5(b)-9(b). Each simulation is done for 2000 seconds. In order to see the effect of the excitation, the excitation begins 100 seconds after the start of the simulation and ends 100 seconds before the simulation ends. The model output voltage drifts towards the resting voltage level in the absence of excitations. A time-dependent decrease in the frequency of the output signal of the model can be seen in Fig.s. 5-9. Four of these simulations are done by giving $\propto$ and β with an increment of 0.2 to demonstrate the behavior of the modified Naguma circuit. In the cases, when α and β values are 0.2 and 0.4, i.e., both of the values are lower than 0.5, the model exhibits fast adaptation behaviour as shown in Fig. 5 and 6. In those cases, when α and β parameters are 0.6 and 0.8, i.e., both of the values are higher than 0.5, the model exhibits slow adaptation behaviour [13]. Therefore, the results seen in Fig.s 5 and 6 can be shown as an example of fast adaptation, whereas the results seen in Fig.s 8 and 9 can be shown as an example of slow adaptation. $\propto= \beta = 0.5$ can almost be regarded as a threshold value between the fast and the slow adaptations. For $\propto= \beta = 0.5$, the simulation result given in Figure 7 shows an intermediate behavior between the fast and slow adaptations. However, it resembles more the slow adaptation behavior seen in Figures 8 and 9.

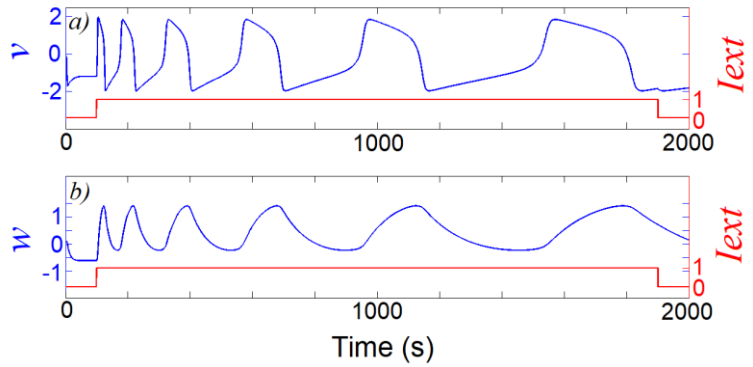

Fig. 5. (a) The external current and the output voltage and (b) the external current and the recovery variable of the modified Nagumo circuit model for $\propto= \beta = 0.2$

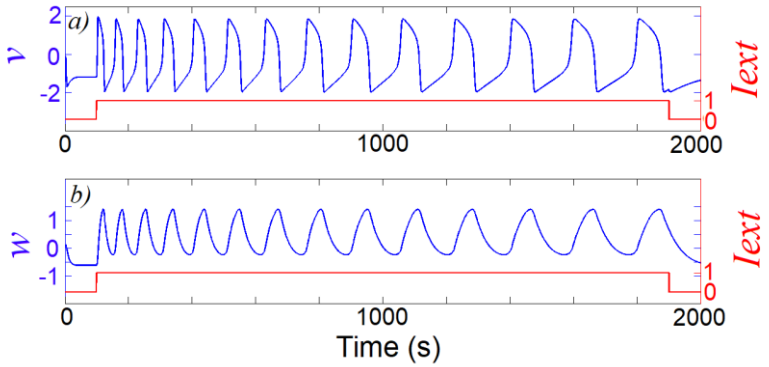

Fig. 6. (a) The external current and the output voltage and (b) the external current and the recovery variable of the modified Nagumo circuit model for $\propto= \beta = 0.4$

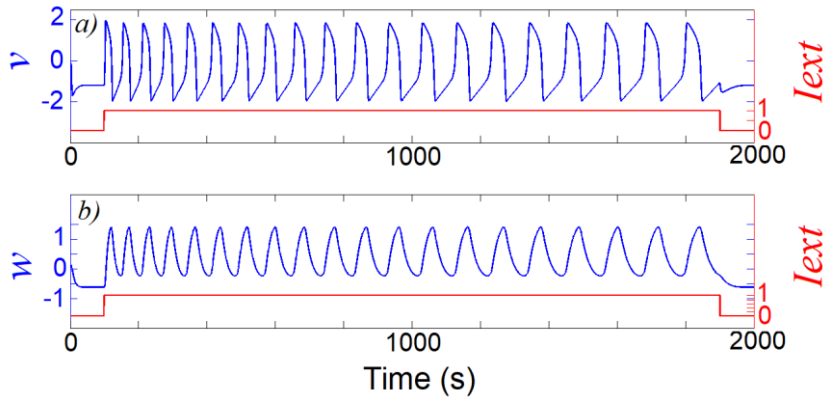

Fig. 7. (a) The external current and the output voltage and (b) the external current and the recovery variable of the modified Nagumo circuit model for $\propto= \beta = 0.5$

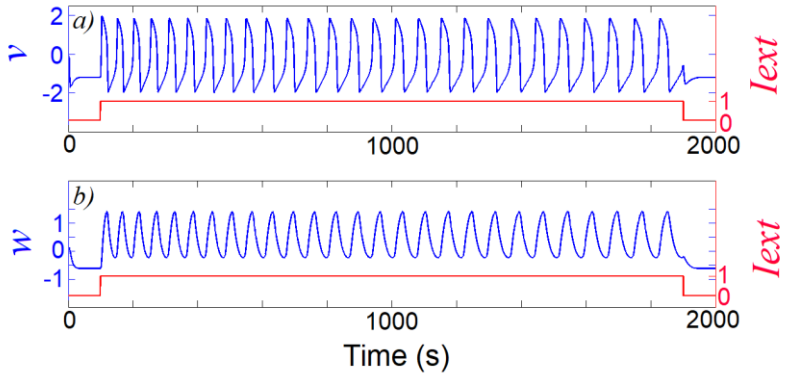

Fig. 8. (a) The external current and the output voltage and (b) the external current and the recovery variable of the modified Nagumo circuit model for $\propto= \beta = 0.6$

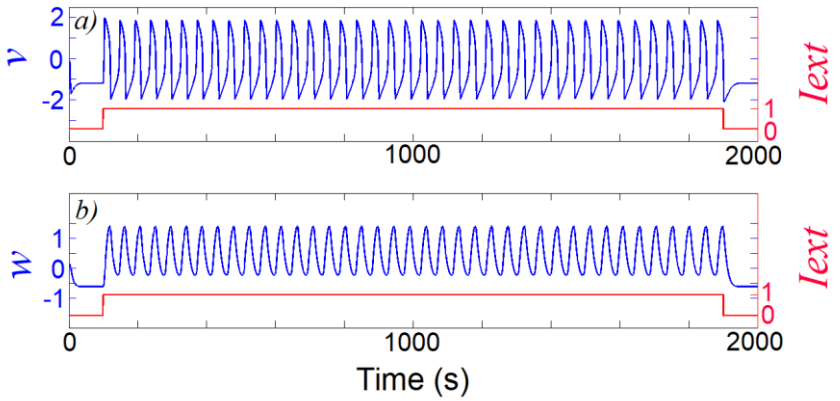

Fig. 9. (a) The external current and the output voltage and (b) the external current and the recovery variable of the modified Nagumo circuit model for $\propto= \beta = 0.8$

In Fig. 10, the variation in the output frequency of the model is given for the simulations seen in Fig.s 5-9. If the α and β parameters are selected higher than *0.5*, slow adaptation can be seen in graphics shown in blue and red in Fig. 10. If the α and β parameters are selected lower than *0.5*, fast adaptation behaviour can be seen in graphics shown in purple and green in Fig. 10. Figure 11 shows the phase plane plot of the CFD-based FHN model. Since the phase relationship of *v* and *w* variables does not change in all cases ($\propto= \beta = 0.2$, 0.4, 0.5, 0.6, and 0.8), the phase plane plot shows the same behaviour. Since the model shows adaptation behaviour, the phase relationship between *v* and *w* parameters does not change for all $\propto= \beta$ values.

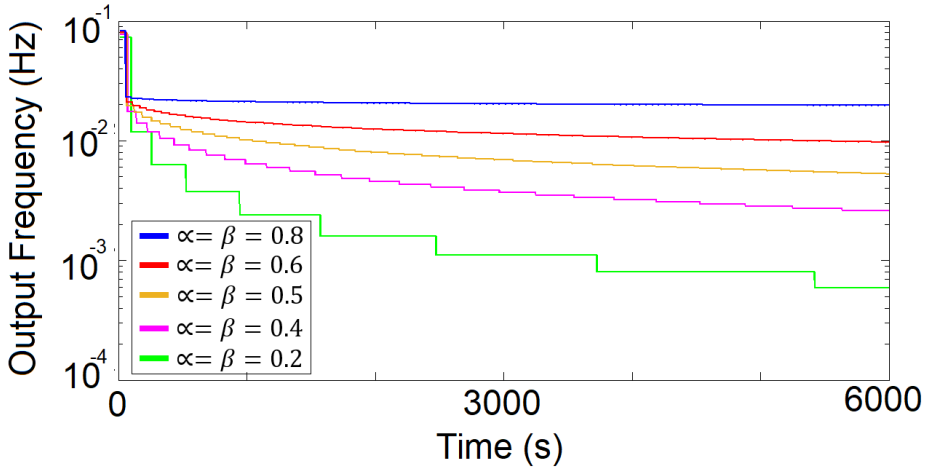

Fig. 10. The output frequency of the modified Nagumo circuit model for the various $\propto = \beta$ values (0.2, 0.4, 0.5 0.6, 0.8)

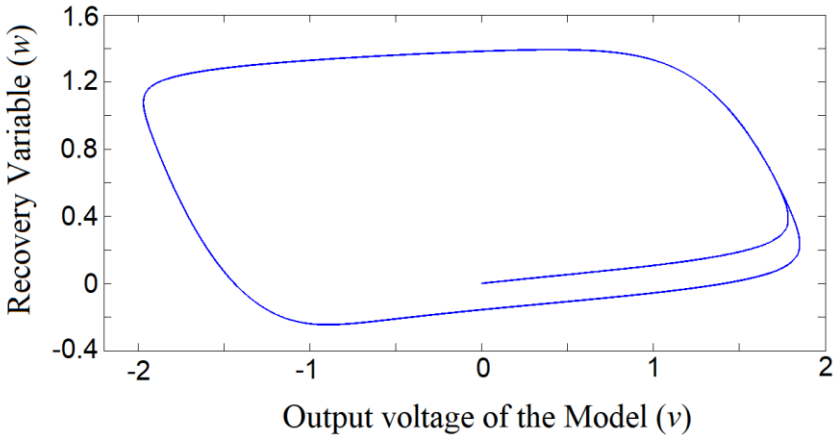

Fig. 11. Phase plane plot of the modified Nagumo circuit model

Figures 12 and 13 show the simulation results when of the $\propto$ and β parameters are not chosen as the same. When $\propto$ is chosen greater than β, the model's behaviour is seen in Fig. 12. Fast adaptation behaviour is observed in this case. However, it can be seen that both the output signal and recovery variable signal have higher slopes in this case. The output voltage rises or falls down very sharply, i.e., gets higher slopes while *w* starts increasing or decreasing as shown in Fig. 12. Following the rise and the fall, the output voltage decreases or increases monotonously respectively. As a result, the output signal *v* has a higher slope at the rising and falling edges. When β is chosen greater than $\propto$, the model's behaviour is seen in Fig. 13. The peak voltage value of the output signal decreases with respect to time and becomes constant at the value of the reverse voltage source *E*. In this case, the output voltage *v* is dragged to the reverse voltage source *E*.

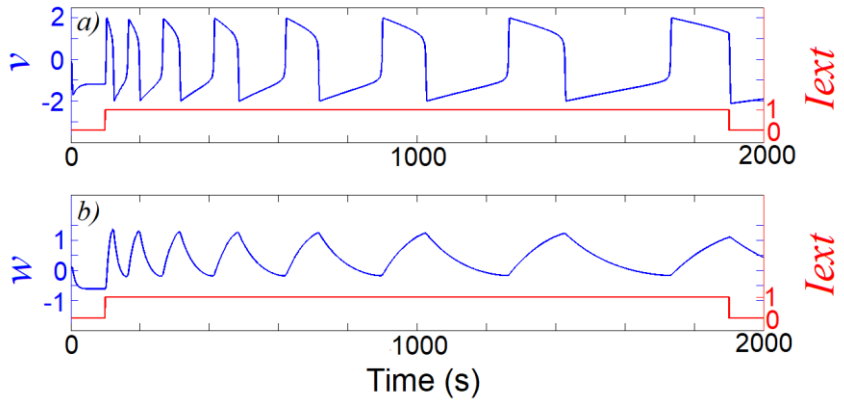

Fig. 12. The external current and the output voltage and b) the external current and the recovery variable of the modified Nagumo circuit model for $\propto$=0.8 and β=0.2

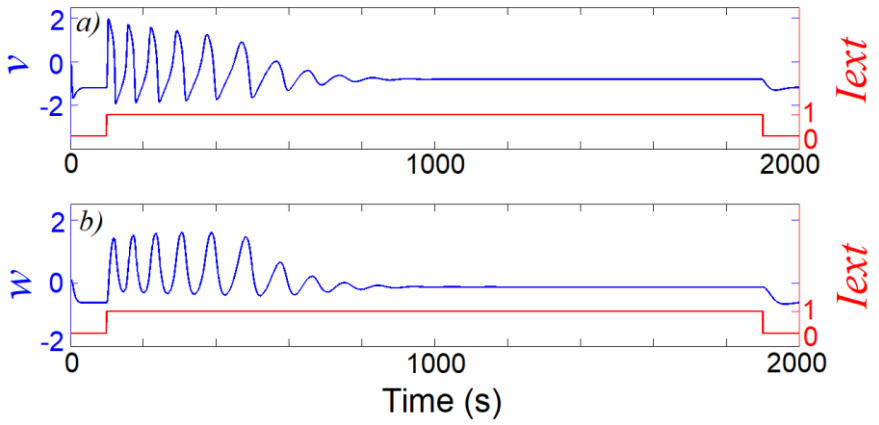

Fig. 13. The external current and the output voltage and b) the external current and the recovery variable of the modified Nagumo circuit model for $\propto$=0.2 and β=0.8

The recovery variable provides negative feedback to the variable *v*. Increases in *w* variable causes the variable *v* to weaken more in this model more than expected from the FHN model. As seen in Fig. 13, the output voltage signal (*v*) becomes constant at the value of the reverse voltage source *E* with the strengthened negative feedback effect of the recovery variable (*w*). This behaviour shown in Fig. 13 is incompatible with the all or nothing principle, which is known as a requirement of neuron electrophysiology.

5. Conclusions

In this study, a FHN model circuit, which possesses a CFD capacitor in parallel with an LTI capacitor and a CFD inductor in series with an LTI inductor, is proposed. The equivalent capacitor and equivalent inductor are time-dependent in this circuit. A method which reset at the beginning of each excitation is proposed in order to prevent time-dependent variation in the absence of excitation in the proposed model. The proposed model shows the adaptation behaviour of biological neuron constant stimulation. The speed of adaptation can be changed by varying the fractional-order degree. Thus, different adaptation behaviours can be modelled. In addition, the anomalies, which occur when the capacitor and inductor fractional degrees are selected differently are also shown and explained through simulations.

It is a well-known fact that, in addition to adaptation, forgetting behaviour is also observed in biological neurons. Accordingly, it is expected that the effects of the first stimulation will be forgotten within a certain time period between two consecutive stimulations. In future studies, the model can be made more specific by adding forgetting behaviour.

Acknowledgement

The author would like to thank Dr. Reşat Mutlu for proofreading.

References

[1] G. Long, G. Fang, “A review of biologically plausible neuron models for spiking neural networks.” *AIAA Infotech@ Aerospace* 2010, vol. 3540, 2010.

[2] W. Gerstner, R. Naud, "How good are neuron models?" *Science*, vol.326, no.5951, p.p. 379-380, 2009.

[3] R. FitzHugh, "Impulses and physiological states in theoretical models of nerve membrane", *Biophysical journal*, vol. 1, no. 6, pp. 445-466, 1961.

[4] J. Nagumo, S. Arimoto, and S. Yoshizawa. "An active pulse transmission line simulating nerve axon." *Proceedings of the IRE* vol. 50, no.10, pp. 2061-2070, 1962.

[5] A. L. Hodgkin, and A. F. Huxley, "A quantitative description of membrane current and its application to conduction and excitation in nerve." *The Journal of physiology*, vol. 117, no. 4, pp. 500-544, 1952.

[6] E. Izhikevich, “Simple Model of Spiking Neurons,” *IEEE Transactions on Neural Networks*, vol. 14, no. 6, pp. 1569-1572, 2003.

[7] Simple Model of Spiking Neurons, [Online]. Available: https://www.izhikevich.org/publications/spikes.htm (Access Date: 28/12/2021).

[8] L. F. Abbott, "Lapicque's introduction of the integrate-and-fire model neuron (1907)" *Brain research bulletin*, vol. 50, no. 5-6, pp. 303-304, 1999.
[9] M. J. Richardson, N. Brunel, and V. Hakim, "From subthreshold to firing-rate resonance." *Journal of neurophysiology* vol. 89, no.5, pp. 2538-2554, 2003.
[10] T. Wondimu, T. M. Marinov, and F. Santamaria, "Neuronal spike timing adaptation described with a fractional leaky integrate-and-fire model." *PLoS computational biology* vol. 10, no.3, pp. e1003526, 2014.
[11] W. Gerstner, W. M. Kistler, R. Naud, and L. Paninski, *Neuronal dynamics: From single neurons to networks and models of cognition*, Cambridge University Press, 2014.
[12] K. G. Pearson, "Neural adaptation in the generation of rhythmic behavior." *Annual review of physiology*, vol. 62, no.1, pp. 723-753, 2000.
[13] S. Chung, X. Li, and S. B. Nelson, "Short-term depression at thalamocortical synapses contributes to rapid adaptation of cortical sensory responses in vivo." *Neuron*, vol.34, no.3, pp. 437-446, 2002.
[14] D. Valério, J. Machado, and V. Kiryakova, "Some pioneers of the applications of fractional calculus", *Fract. Calc. Appl. Anal.*, vol.17, no.2, pp.552–578, 2014.
[15] S.M. Shah, R. Samar, N. M. Khan, and M. A. Z. Raja, "Fractional-order adaptive signal processing strategies for active noise control systems." *Nonlinear Dynamics*, Vol. 85, pp. 1363–1376, 2016.
[16] D. del-Castillo-Negrete, B. A. Carreras, and V. E. Lynch, "Fractional diffusion in plasma turbulence." *Physics of Plasmas*, vol. 11, no. 8, pp. 3854-3864, 2004.
[17] V.E. Tarasov, "Review of some promising fractional physical models." *International Journal of Modern Physics B*, vol. 27, no.09, pp. 1330005, 2013.
[18] M. Caputo, "Linear Models of Dissipation whose Q is almost Frequency Independent II", *Geophysical Journal International*, vol. 13, no. 5, pp. 529–539, 1967.
[19] R. Agarwal, M. Belmekki, and M. Benchohra. "A survey on semilinear differential equations and inclusions involving Riemann-Liouville fractional derivative." *Advances in Difference Equations*, vol. 2009, pp. 1-47, 2009.
[20] R. Scherer, S. L. Kalla, Y. Tang, and J. Huang, "The Grünwald–Letnikov method for fractional differential equations." *Computers & Mathematics with Applications*, vol. 62, no.3, pp. 902-917, 2011.
[21] R. Khalil, M. A. Horani, A. Yousef, and M. Sababheh, "A new definition of fractional derivative." *Journal of computational and applied mathematics*, vol. 264, pp. 65–70, 2014.
[22] T. Abdeljawad, T. "On conformable fractional calculus." *Journal of computational and Applied Mathematics*, vol. 279, pp. 57-66, 2015.
[23] A. O. Akdemir, H. Dutta, and A. Atangana, eds. *Fractional order analysis: theory, methods and applications*. John Wiley & Sons, 2020.
[24] R. Sikora, R. "Fractional derivatives in electrical circuit theory–critical remarks." *Archives of Electrical Engineering*, vol. 66, no. 1, pp. 155-163, 2017.
[25] T. J. Anastasio, "The fractional-order dynamics of brainstem vestibulo-oculomotor neurons." *Biological cybernetics*, vol. 72, no. 1, pp. 69-79, 1994.
[26] K. Moaddy, A. G. Radwan, K. N. Salama, S. Momani, and I. Hashim, "The fractional-order modeling and synchronization of electrically coupled neuron systems." *Computers & Mathematics with Applications*, vol. 64, no.10, pp. 3329-3339, 2012.
[27] M. Yavuz, B. Yaşkıran, "Conformable Derivative Operator in Modelling Neuronal Dynamics." *Applications & Applied Mathematics*, vol. 13, no.2, 2018.
[28] M. Armanyos, A. G. Radwan. "Fractional-order Fitzhugh-Nagumo and Izhikevich neuron models." *2016 13th international conference on electrical engineering/electronics, computer, telecommunications and information technology (ECTI-CON)*, pp. 1-5, 2016.
[29] L. Martínez, J. J. Rosales, C. A. Carreño, and J. M. Lozano, "Electrical circuits described by fractional conformable derivative." *International Journal of Circuit Theory and Applications*, vol. 46, no.5, pp. 1091-1100, 2018.
[30] U. Palaz, R. Mutlu, "Analysis of a Capacitor Modelled with Conformable Fractional Derivative Under DC and Sinusoidal Signals." *Celal Bayar University Journal of Science*, vol. 17, no. 2, p. p. 193-198, 2021.
[31] A. Petrovas, S. Lisauskas, and A. Slepikas. "Electronic model of fitzhugh-nagumo neuron." *Elektronika Ir Elektrotechnika*, vol. 122, no .6, pp. 117-120, 2012.
[32] M. Chen, J. Qi, Q. Xu, and B. Bao, "Quasi-period, periodic bursting and bifurcations in memristor-based FitzHugh-Nagumo circuit." *AEU-International Journal of Electronics and Communications*, vol. 110, pp. 152840, 2019.
[33] E. M. Izhikevich, R. FitzHugh, "FitzHugh-nagumo model." *Scholarpedia*, vol. 1, no. 9, p. p. 1349, 2006.
[34] T. Kanamaru, "Van der Pol oscillator." *Scholarpedia* vol. 2, no. 1 pp. 2202, 2007.

Author biography

Ertuğrul Karakulak (PhD) was born in Tekirdağ, Turkey in 1979. He received B.Sc. degree from Sakarya University in Electronics Education in 2001, M.Sc degree in 2005 and Ph.D. degree from Trakya University in 2016. He is currently an assistant professor at the Biomedical Device Technology Department, Vocational School of Technical Sciences, Tekirdağ Namik Kemal University. His research interests include memristors, resistive RAMs, fractional order derivatives, and microcontrollers.